



P2X₇ receptor in the hippocampus is involved in gp120-induced cognitive dysfunction

Y. Liu^{1*}, G.Q. Chen^{1*}, B.Y. Liu^{1*}, Q. Chen^{3*}, Y.M. Qian², S.S. Qin³,
C.L. Liu³ and C.S. Xu³

¹The First Clinical Medical College, Nanchang University, Nanchang, China

²Nursing College, Nanchang University, Nanchang, China

³Department of Physiology, Basic Medical College, Nanchang University, Nanchang, China

*These authors contributed equally to this study.

Corresponding author: C.S. Xu

E-mail: xuchangshui@ncu.edu.cn

Genet. Mol. Res. 16 (1): gmr16019356

Received September 21, 2016

Accepted September 21, 2016

Published January 23, 2017

DOI <http://dx.doi.org/10.4238/gmr16019356>

Copyright © 2017 The Authors. This is an open-access article distributed under the terms of the Creative Commons Attribution ShareAlike (CC BY-SA) 4.0 License.

ABSTRACT. To investigate the role of the P2X₇ receptor in learning and memory dysfunction induced by HIV-1 envelope glycoprotein gp120 (gp120), we established HIV-1-associated dementia (HAD) animal models by intracerebroventricular (ICV) infusion of gp120 in rats. We observed gp120-induced cognitive dysfunction in the radial arm water maze test. Results showed that rats in the gp120 groups had longer escape latencies and more errors compared to those in the control group. For example, the average trial time in the 50-ng/day-gp120 group on day eight (16.57 ± 1.71 s, N = 90) was significantly longer than that of control rats (9.93 ± 0.68 s, N = 90). The relative expression of P2X₇ mRNA in the control, 50-, 70-, and 100-ng/day-gp120 groups were 0.43 ± 0.06 , 0.48 ± 0.07 , 0.83 ± 0.05 , and 0.84 ± 0.10 , respectively; relative P2X₇ protein expression in those groups

was 0.63 ± 0.07 , 1.08 ± 0.06 , 0.90 ± 0.07 , and 1.03 ± 0.11 , respectively. According to immunohistochemistry analysis, the staining intensity values for P2X₇ protein expression in the control, 50-, 70-, and 100-ng/d-gp120 groups were 0.88 ± 0.07 , 1.41 ± 0.12 , 1.28 ± 0.13 , and 1.31 ± 0.10 , respectively. The above results showed that the expression of P2X₇ increased significantly in the hippocampus of gp120 rats compared to that of the control group. These results suggest that ICV infusion of gp120 can successfully mimic HAD in rats, and P2X₇ may be involved in gp120-induced cognitive dysfunction. This could provide a theoretical foundation and potential drug target for research and treatment of ADC.

Key words: HIV-1 associated dementia; Learning and memory deficits; Gp120; P2X₇ receptor

INTRODUCTION

The incidence of nervous system diseases among late-stage AIDS and HIV-infected patients varies between 15 and 20% (Yilmaz et al., 2012). The core symptoms of HIV-associated dementia (HAD), also referred to as AIDS-dementia complex (ADC), include cognitive impairment (such as learning and memory dysfunction), movement disorders, and psychological and behavioral abnormalities, and is thus a serious issue (Peluso and Spudich 2014; Zayyad and Spudich 2015). Researchers have found that activation of macrophages/microglia is critical for the occurrence of ADC; however, the specific mechanisms remain unclear. Various harmful substances can be produced by activated macrophages/microglia, which can damage the central nervous system (CNS) and induce apoptosis and neurodegenerative disease. In fact, excessive activation of microglia is one of the most significant known causes of neuroinflammation (Glass et al., 2010; Krogh et al., 2014; Zhao et al., 2014). In addition, results from animal experiments have elucidated important information about ADC. For example, intracerebroventricular (ICV) injection of HIV-1 envelope glycoprotein gp120 (gp120) into the adult rat was suggested to have serious destabilizing effects on the brain (Potter et al., 2013). In addition, adenosine 5'-triphosphate (ATP), released by damaged neural cells, can stimulate stellate cells to release ATP and other chemical compounds (Cunningham 2013). The P2X₇ receptor can then initiate microglial chemoattraction induced by ATP. This contributes to microglial proliferation and chronic inflammation of neural cells by stimulating the release of neurotoxic inflammatory factors (Huang et al., 2015).

Based on these observations, we investigated if P2X₇ receptors in the hippocampus are involved in ADC induced by gp120 through ICV infusion. We found that gp120 could reduce learning and memory and increase the expression of P2X₇ receptor in the rat hippocampus, suggesting that P2X₇ receptor might play an important role in gp120-induced learning and memory deficits. The findings presented here might be of considerable significance for understanding the potential role of P2X₇ in the pathogenesis of ADC and for exploring novel targets for ADC prevention and treatment.

MATERIAL AND METHODS

Animal grouping and experimental design

This study was performed from January 2014 to November 2015 at the Basic Medical College of Nanchang University. All procedures were carried out under strict scrutiny and supervision to ensure they conformed to stipulations of Nanchang University and the ethical guidelines set by the Ethical Committee of the Nanchang University (which is based on the National Institutes of Health Guide for the Care and Use of Laboratory Animals). Healthy Sprague-Dawley (SD) rats (135-175g, with an equal number of males and females) were supplied by the Center of Laboratory Animal Science of Nanchang University. The SD rats were randomly divided into control (Ctrl), 50 ng/day gp120 (gp120 50ng), 70 ng/day gp120 (gp120 70ng), and 100ng/day gp120 (gp120 100ng) groups, each of which included six animals. The rats were fed in plastic cages at 21°-25°C and were acclimated to the laboratory environment for one week before behavioral testing.

Establishment of HAD model

Before the surgical procedure using a brain stereotaxic apparatus (NEST Biotechnology Co. Ltd.), we used 10% chloral hydrate (0.3-0.35 mg/kg) to anesthetize rats with intraperitoneal (*ip*) injection. The fur on the rat's head was removed, the scalp was disinfected, and a 2-cm incision was made in the middle of the top of the head, exposing the anterior fontanel. According to the rat orthostatic brain atlas, the animal's skull was opened with a dental drill of 2.0 mm; stereotaxic coordinates for the LV were anterior/posterior: -1.0 mm, medial/lateral: ±1.5 mm, and dorsal/ventral: -3.5 mm from the bregma; a sterilized polyethylene plastic tube was then immediately inserted into the skull and fixed with dental powder (Keblesh et al., 2009; Fornari et al., 2012). The head skin was disinfected with iodine and the incision was then sutured. Amoxicillin was administered daily to prevent infection. The ICV was left untouched in the Ctrl group, and rats not receiving the operation served as a normal control. ICV infusion was performed starting on the fourth day after stereotaxic surgery was restored, during which rats were anesthetized with ether and infused perpendicular to the scalp. Rats in the gp120 groups received ICV infusion of 5 µL gp120 (Sigma, USA) daily for three days, at a speed of 0.5 µL/min for five minutes before slowly removing the needle (Tang et al., 2009).

Radial arm water maze (RAWM) behavior test

A six-arm radial water maze apparatus was used to test the behavior changes (provided by Shenzhen Wald Company; diameter: 120 cm, height: 110 cm, water depth: 25 cm). This experimental device contains a target platform (13 x 13 cm) which located in a movable arm and 2 cm below water level, and the rats can obtain spatial orientation from a fixed light source and intra-maze visual cues. Room temperature was maintained at 22°C, and water temperature was maintained at and 17°-22°C (Keblesh et al., 2009; Mika et al., 2012). A 3-day protocol, which consist of five blocks of three trials each (a total of 15 trials per day), was conducted after ICV 1 week and 2 weeks, respectively. The amount of time required to discover the hidden platform (escape latency) and incorrect arm choices (errors) were recorded during each 60-s trial, and the rat still remained on the platform for 15 s after successfully found the

target platform. In consideration of extended periods of rest between blocks, experimental rats were swimming in cohorts of three for each block. For the 1st week, the target quadrant for each animal was randomly assigned and fixed for a particular 3-day protocol to evaluate spatial learning and memory, whereas the initial quadrant varied randomly for each trial. For the 2nd week, each rat was randomly assigned a different target quadrant to evaluate new spatial learning and memory; before the experiment, rats received the same training (Keblesh et al., 2009; Tang et al., 2009).

Reverse transcriptase-PCR (RT-PCR)

After the RAWM experiment, the rats were anesthetized and the hippocampus was removed after decapitation. RT-PCR was then used to detect the expression of P2X₇ mRNA in the hippocampus. Total RNA was extracted with a Total RNA Isolation Kit (Invitrogen) and PCR amplification was undertaken after reverse transcription (RT) reaction. The upstream primer and downstream primer sequences of the P2X₇ mRNA were 5'-CACCCGCGAGTACAACCTTC-3', and 5'-CCCATACCCACCATCACACC-3', respectively, and product size was 225 bp. β -actin, as an internal control, and was amplified using specific primers (forward and reverse primer sequence were 5'-CACCCGCGAGTACAACCTTC-3' and 5'-CCCATACCCACCATCACACC-3', respectively with a product size of 240 bp). UV was applied for DNA band detection and photographs were taken; a gel imaging system was used to obtain the spot density scanning value of the objective electrophoresis bands. The Gel Imaging System software (Junyi, Shanghai, China) was used to analyze band densities and the relative expression of P2X₇ mRNA was calculated after normalized to each β -actin internal control. PCR was performed in over 30 cycles, with the RT reaction being undertaken at 50°C for 15 min and the RTase inactivation being undertaken at 94°C for 2 min, followed by denaturation at 94°C for 30 s, annealing at 60°C for 30 s, and final extension at 72°C for 1.5 min.

Quantitative real-time PCR (qPCR)

To confirm RT-PCR results, P2X₇ mRNA expression was assessed by qPCR. After extraction, total RNA was quantified by determining its optical density at 260 nm; 25 ng total RNA was then reverse transcribed. SYBR[®] Green real-time PCR, using the ABI PRISM[®] 7500 Sequence Detection System (Applied Biosystems Inc., Foster City, CA, USA) was performed to quantify the expression of P2X₇ at the mRNA level. For PCR amplification, 2 μ L cDNA was used in a total volume of 20 μ L, and each sample was assayed in triplicate. The upstream and downstream primer sequences for P2X₇ were 5'-GAGCACGAATTATGGCACCG-3' and 5'-TAACAGGCTCTTTCCGCTGG-3', respectively, and the expected product size was 107 bp. The expression level of β -actin was determined as a reference through amplification using specific primers (the primer sequences of forward and reverse were 5'-GGAGATTACTGCCCTGGCTCCTA-3' and 5'-GACTCATCGTACTCCTGCTTGCTG-3', respectively). The expected product size was 150 bp. Cycling parameters were as follows: 94°C for 30 s to activate DNA polymerase, 40 cycles of 94°C for 5 s and 60°C for 30 s for amplification; 95°C for 15 s, 60°C for 1 min, and 95°C for 15 s to obtain the melt curve. The average threshold cycle (CT) value for β -actin was subtracted from the average P2X₇ value to yield the CT value (CT = CT target - CT reference). The $\Delta\Delta$ CT parameter was calculated as follows: CT = CT test sample - CT calibrator sample. The relative expression levels of P2X₇ (RQ) were compared to those of the independent groups using the following equation: $RQ = 2^{-\Delta\Delta CT}$.

Western blot

After the water maze experiment, the rats were anesthetized with 10% chloral hydrate, decapitated, and the hippocampus was removed. Tissues from each group were placed in the spherical portions of 2 mL homogenizer, homogenized with 1 mL RIPA lysis buffer (containing PMSF), and then put on ice and ground repeatedly until the sample was fully crushed. The homogenate lysates were centrifuged at 4°C at a speed of 12,000 rpm for 10 min and the supernatant was harvested, then Lowry method was used to evaluate the total protein concentration. After diluting with 6X protein loading buffer, and heating to 95°C for 10 min, samples containing equal amounts of protein (20 µg) were separated by SDS-polyacrylamide gel (10%) electrophoresis using an electrophoresis apparatus (Liuyi Beijing Instrument Factory, China). Protein was then transferred to PVDF membranes using the same system. Chemiluminescent signals were observed using the multifunctional gel imaging system (Bio-Rad Company, USA), and band intensity was quantified using the Image-Pro Plus 6.0 software (Media Cybernetics, USA). The antibodies and their dilutions were as follows: rabbit polyclonal anti-P2X₇ (Abcam, USA; 1:1000 dilution), monoclonal β-actin (Beijing Zhongshan Biotech Co., China; 1:800 dilution), and secondary antibody (Beijing Zhongshan Biotech Co., China; 1:2000 dilution). The relative expression of P2X₇ protein was calculated after normalized to each β-actin internal control.

Immunohistochemistry

Immunohistochemical staining was performed using an SP-9001 kit (Beijing Zhongshan Biotech Co., China) according to the manufacturer instructions. Briefly, after RAWM tests, the hippocampus was isolated from each rat and washed with phosphate buffered saline (PBS). The hippocampus tissue was cut into 20-µm thick sections using a cryostat after being fixed with 4% paraformaldehyde for 24 h and dehydrated with 20% sucrose overnight at 4°C. The tissue slice was incubated with 3% H₂O₂ for 15 min to block endogenous peroxidase activity after washing with PBS for three times, then blocking non-specific antigens with 10% goat serum for 40 min at room temperature. The tissue slice was incubated with rabbit anti-P2X₇ (Abcam, USA; 1:300 diluted in PBS) overnight at 4°C. The stain intensity values (average optical density) of P2X₇ in the hippocampus were analyzed by an image scanning analysis system (HMIV-2000, Wuhan, China), and the background of P2X₇ receptor expression was determined by averaging the optical density of ten random areas.

Statistical analysis

Statistical analyses were performed using SPSS 21.0 (IBM, USA). All data are reported as means ± SE. Statistical significance was determined by analysis of variance (ANOVA), followed by an LSD test for multiple comparisons between group pairs. P < 0.05 was considered significant. Graphs were prepared using the SigmaPlot 12.0 software (Systat Software Inc., USA).

RESULTS

Effect of different doses of gp120 on spatial learning and memory in rats

After groups of rats were infused continuously with different doses of gp120 (50, 70,

and 100 ng/day) for three days, a 3-day protocol was performed starting on the 6th day (the 6th-8th days after gp120 ICV perfusion for three days). Repeated measure ANOVA showed that the effect of time (within-subjects factors) was statistically significant ($F_{2,712} = 344.438$, $P < 0.001$, for the escape latency; $F_{2,712} = 28.501$, $P < 0.001$, for the number of errors). As shown in Figure 1, the escape latency and target platform errors for each group (between-subjects factors) reduced gradually with increased water maze testing, indicating that rats had formed a certain amount of learning and memory that helped them to find the target platform. There was an interaction between time and gp120 factors for escape latency ($F_{6,712} = 22.961$, $P < 0.001$) and the number of errors ($F_{6,712} = 6.353$, $P < 0.001$). Based on the ANOVA results, the escape latency for each group was statistically significant ($F_{3,356} = 241.775$, $P < 0.001$); similar results were also obtained for the number of errors ($F_{3,356} = 28.425$, $P < 0.001$). Based on LSD test results, gp120 infusion (50, 70, 100 ng/day) significantly prolonged escape latency and increased target platform errors compared to those parameters in Ctrl rats ($P < 0.05$ or 0.01); the maximum effect was observed in the 100-ng/day treatment group ($P < 0.01$, Figure 1). For instance, the average time (17.50 ± 0.67 s, $N = 18$, Figure 1A) and the average number of errors (2.10 ± 0.17 errors, $N = 18$, Figure 1C) to find the target platform in block five on the 6th day were significantly ($P < 0.05$) higher in gp120 50ng rats than in Ctrl rats (15.0 ± 1.45 s, $N = 18$; 1.20 ± 0.22 errors, $N = 18$), suggesting an injury of spatial learning and memory in this group. Likewise, compared to the Ctrl group, the gp120 groups exhibited a significantly longer escape latency (Figure 1B; $P < 0.05$ or 0.01) for all three testing days 1 week after perfusion. For example, the average trial time of gp120 50ng rats on day eight (16.57 ± 1.71 s, $N = 90$) was significantly longer than that of Ctrl rats (9.93 ± 0.68 s, $N = 90$; $P < 0.01$).

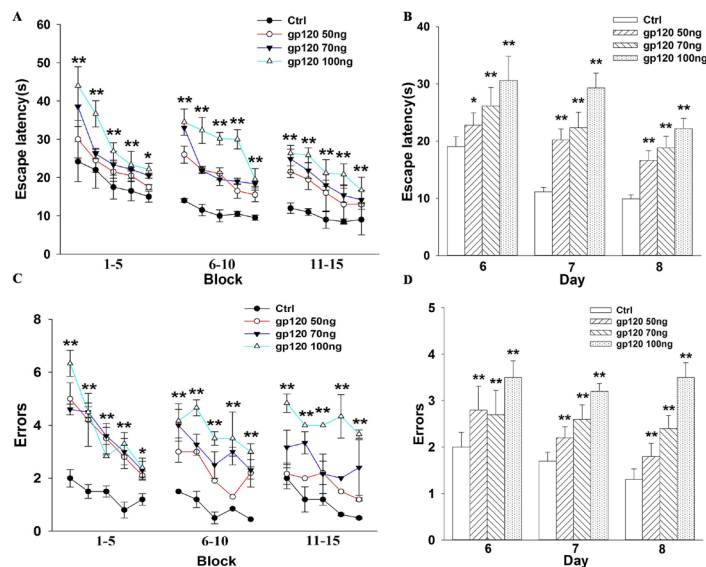


Figure 1. Different doses of gp120 could decrease spatial learning and memory in rats. A 3-day protocol, which consist of five blocks of three trials each (a total of 15 trials per day), was conducted on each group (consisting of six rats) during the first week post-infusion. Three days after injection, escape latency (A and B) and errors (C and D) indicated slower learning and decreased interday memory in gp120 animals compared to those of the controls. Daily analysis revealed sizable deficits in escape latency and errors in gp120 rats at week one after infusion. All data are reported as means \pm SE. * $P < 0.05$, ** $P < 0.01$, versus Ctrl group.

New learning and memory of rats decreased after continuous gp120 ICV perfusion

We then determined whether the detrimental effect of gp120 receded new learning and memory. At the end of the former experiment, we performed the 3-day protocol on the 13th-15th days after continuous ICV perfusion of gp120 for three days. The effect of time was statistically significant ($F_{2,712} = 317.111$, $P < 0.001$, for the escape latency; $F_{2,712} = 98.158$, $P < 0.001$, for the number of errors, as shown in Figure 2), and there was an interaction between time and gp120 factors for escape latency ($F_{6,712} = 5.000$, $P < 0.001$) and the number of errors ($F_{6,712} = 19.414$, $P < 0.001$). Based on ANOVA results, the escape latency for each group was statistically significant ($F_{3,356} = 154.853$, $P < 0.001$); similar results were obtained for the number of errors ($F_{3,356} = 138.337$, $P < 0.001$). For example, on the 13th day of testing, both escape latency and errors were higher for groups treated with different doses of gp120 compared to those of the Ctrl (Figure 2B, D; $P < 0.01$). Furthermore, the results of the 2nd and 3rd testing days of week two were analogous to the week one, suggesting persistent gp120-related damage. Observably, the escape latency time and errors for groups on each day of the 2nd week of testing receiving different doses of gp120 were higher than those of the Ctrl group ($P < 0.01$). For instance, the average escape latency for gp120 50ng rats on the 15th day of the 2nd week was 15.60 ± 3.71 s ($N = 90$), which was significantly higher than that of the Ctrl group (8.90 ± 2.68 s, $N = 90$, Figure 2B; $P < 0.01$). From the above, these behavior analyses indicated deficits in learning and memory, and demonstrated significant impaired the scores of learning and memory in response to gp120 treatment.

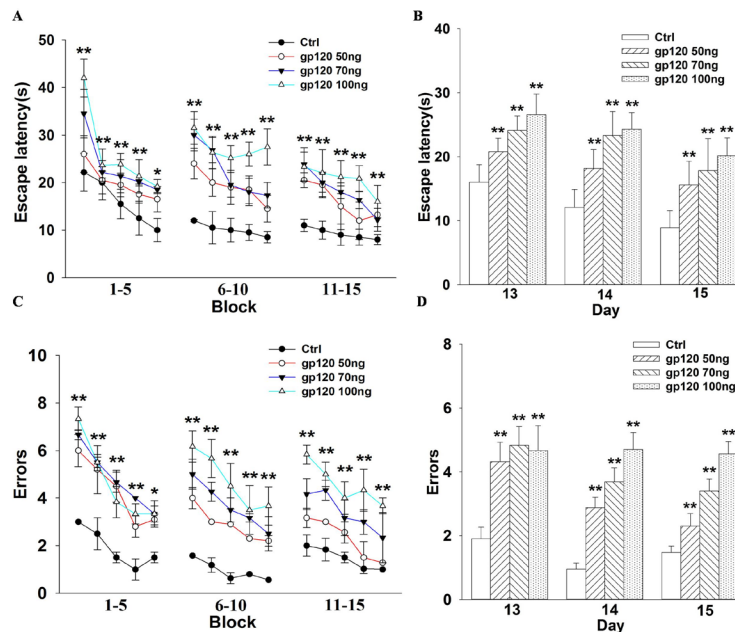


Figure 2. New learning and memory in rats decreased after continuous gp120 ICV perfusion. A 3-day protocol was performed during the second week after infusion. Gp120-treated rats showed longer escape latency (A and B) and made more errors (C and D) compared to Ctrl group rats. Day analysis revealed evident deficits (in both escape latency and errors) in gp120-treated animals at week two after inoculation, as well as in the Ctrl group. All data are reported as means \pm SE. * $P < 0.05$, ** $P < 0.01$, versus the Ctrl group.

P2X₇ mRNA in rats was significantly increased by gp120 treatment

Results showed that the relative P2X₇ mRNA expression (based on normalizing to β -actin expression) in the hippocampus of rats from Ctrl, gp120 50ng, gp120 70ng, and gp120 100ng groups was 0.43 ± 0.06 , 0.48 ± 0.07 , 0.83 ± 0.05 , and 0.84 ± 0.10 , respectively. Statistical analysis indicated that the variance was significant ($F_{3,20} = 34.958$, $P < 0.001$; Figure 3). Based on an LSD test, P2X₇ mRNA expression in both the gp120 70ng and gp120 100ng groups was significantly higher than that of the Ctrl group ($P < 0.01$). To ensure consistency of the results, we repeated the experiment using qPCR; the results were similar to those of RT-PCR ($F_{3,20} = 93.438$, $P < 0.001$; Figure 4). Based on the results obtained, we concluded that the expression of P2X₇ mRNA was upregulated in rats with gp120-induced learning and memory deficits.

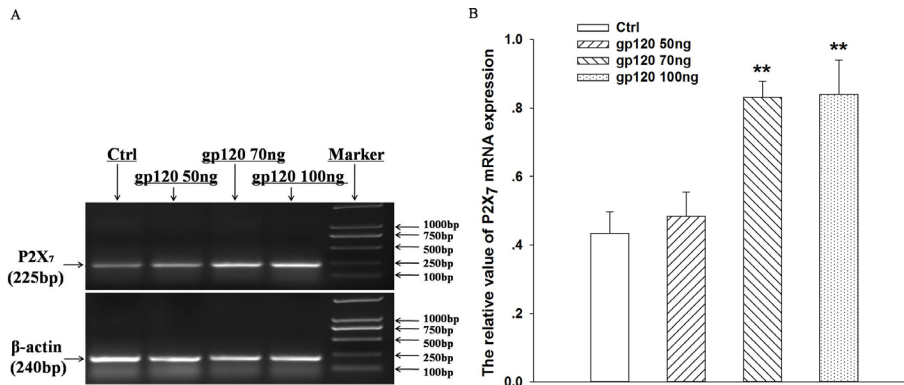


Figure 3. Expression of P2X₇ mRNA was upregulated in the hippocampus of rats with gp120-induced learning and memory deficits. **A.** Representative agarose gel electrophoresis of RT-PCR products for hippocampus P2X₇ mRNA and β -actin. **B.** Relative expression of P2X₇ mRNA in each group via RT-PCR. All experiments were conducted in triplicate. Data are reported as means \pm SE. ** $P < 0.01$, versus Ctrl group.

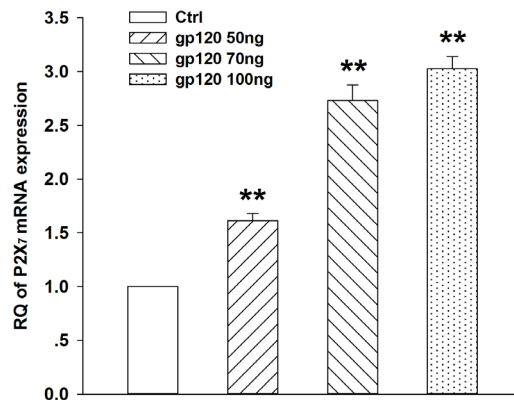


Figure 4. Expression of P2X₇ mRNA was upregulated in the hippocampus of rats with gp120-induced learning and memory deficits based on qPCR. All experiments were conducted in triplicate. Data are reported as means \pm SE. ** $P < 0.01$, versus Ctrl group.

P2X₇ receptor protein was significantly increased by gp120 treatment

The ratio of band intensity of P2X₇ to corresponding β -actin was considered the relative amount of protein expression. The relative expression of P2X₇ protein in the rat hippocampus of Ctrl, gp120 50ng, gp120 70ng, and gp120 100ng groups was 0.63 ± 0.07 , 1.08 ± 0.06 , 0.90 ± 0.07 , and 1.03 ± 0.11 , respectively, and the variance was statistically significant ($F_{3,20} = 18.083$, $P < 0.001$). Further analysis indicated that the expression of P2X₇ protein in the gp120-treated groups was significantly higher than that of the Ctrl group ($P < 0.05$ or 0.01 , Figure 5), suggesting upregulation of this protein in response to gp120-induced learning and memory deficits.

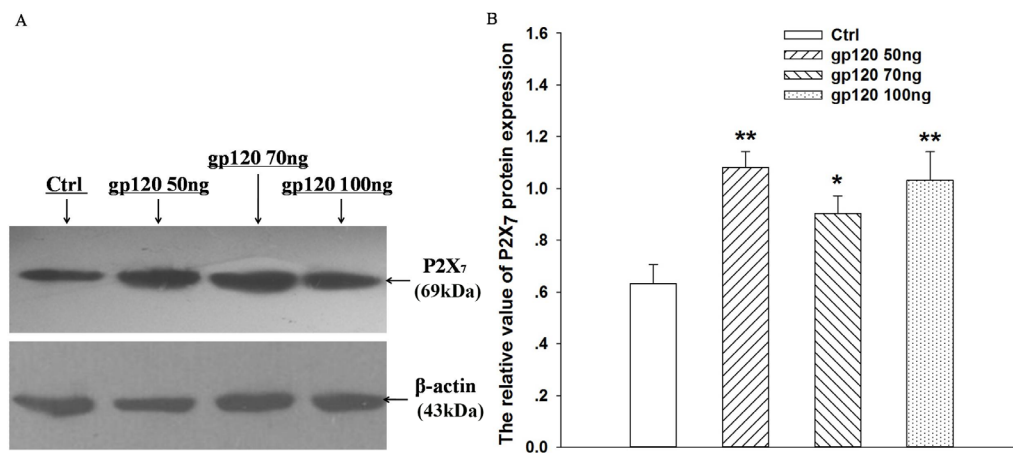


Figure 5. Expression of hippocampus P2X₇ receptor was upregulated in rats with gp120-induced learning and memory deficits. **A.** Representative western blots for expression of P2X₇ receptor (69 kDa) in the hippocampus using β -actin (43 kDa) internal control in the same samples. **B.** Relative expression level of hippocampus P2X₇ receptor protein in each group. All experiments were conducted in triplicate and data are reported as means \pm SE. * $P < 0.05$, ** $P < 0.01$, versus Ctrl group.

Upregulation of P2X₇ immunoreactivity in response to gp120 treatment

To further investigate the role of the P2X₇ receptor in gp120-induced learning and memory deficits, P2X₇ receptor immunoreactivity was assessed via immunohistochemistry. According to image analysis, the staining intensity values (average optical density) for P2X₇ in the Ctrl, gp120 50ng, gp120 70ng and gp120 100ng groups were 0.88 ± 0.07 , 1.41 ± 0.12 , 1.28 ± 0.13 , and 1.31 ± 0.10 , respectively, and the variance was statistically significant ($F_{3,20} = 5.107$, $P = 0.009 < 0.01$; Figure 6). Statistical analysis indicated that the staining intensity value in the gp120 50ng, gp120 70ng, and gp120 100ng rats was significantly higher than that of Ctrl rats ($P < 0.05$ or 0.01). These results indicate that gp120 can upregulate the expression of P2X₇ in the hippocampus of rats.

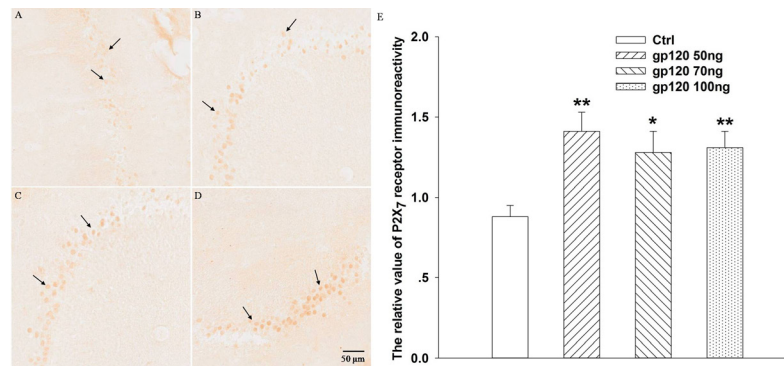


Figure 6. Immunoreactivity of P2X₇ in the hippocampus was upregulated by gp120. Representative results of P2X₇ receptor expression are shown as: **A.** Ctrl group; **B.** gp120 50ng group; **C.** gp120 70ng group; **D.** gp120 100ng group; **E.** relative expression level of the P2X₇ receptor in the hippocampus of each group based on immunohistochemistry. The horizontal line indicates the scale bar (50 μ m). Arrows indicate immunoreactive (positive) cells. All data are reported as means \pm SE (N = 6). *P < 0.05, **P < 0.01, versus Ctrl group.

DISCUSSION

Presently, there are more than 35 million individuals worldwide suffering from HIV/AIDS (Bachani et al., 2013; Ruelas and Greene 2013; Maartens et al., 2014). HIV infection can lead to ADC/HAD, a serious complication of the nervous system (Chen et al., 2011; Yilmaz et al., 2012; Thomas et al., 2013). HAD contributes to functional deficits such as learning and memory decline, cognitive and reasoning dysfunction, inattention, impaired motor skills, and abulia, among others (Singer et al., 2010; Rosca et al., 2012; Peluso and Spudich 2014). More importantly, gp120 can activate macrophages resulting in the production of copious amounts of chemokines/cytokines, and can also influence glutamate uptake in astrocytes and interfere with the glutamine supply for neurons, severely impacting learning and memory (Hazleton et al., 2010; Ogden and Traynelis 2011; Fields et al., 2014). Through behavioral testing in the first week, we found that the average escape latency and number of errors in gp120-treated groups were higher than those of Ctrl rats, indicating that gp120 affected learning and memory in rats. In the second week, gp120-treated rats failed to find the target platform more often compared to control rats, further indicating that different doses of gp120 could reduce learning and memory in rats, and that ICV perfusion of gp120 effectively imitates HAD animal model. Gp120, a surface-expressed glycoprotein of the HIV envelope, is essential for virus entry into cells and plays a vital role in the attachment to specific cell surface receptors (de Witte et al., 2007). Some limitations exist in our HAD animal model based on ICV infusion of gp120, and thus this model does not perfectly represent ADC. For example, different toxic proteins (for example, Tat, Vpr, and Nef) and envelope glycoprotein (gp120 and gp41) of the HIV virus could be involved in the CNS impairment (Dugas et al., 2000; Bodner et al., 2002). This needs to be addressed in future research. Taken together, these results suggest that HIV-1 gp120, a neurotoxin, likely causes toxicity and apoptosis in neurons, and might directly lead to cognitive impairment (Sacktor et al., 2007; Gong et al., 2012; Bartesaghi et al., 2013).

The P2X receptor is an ATP ion channel, and seven types of P2X₁₋₇ ligand gated ion channels have been identified to date (Burnstock 2009; Ortega et al., 2011). P2X receptors are widespread throughout the body, they can be found in the digestive, respiratory,

cardiovascular, genitourinary, nervous, and musculoskeletal systems (Arulkumaran et al., 2011; Trang et al., 2012). The P2X₇ receptor differs significantly from other P2X receptor subtypes, as the interaction between ATP and P2X₇ receptors can activate multiple intracellular signaling pathways involved in immune reactions, neurotransmitter release, oxidative stress, cell proliferation, and apoptosis (Surprenant and North 2009; Zou et al., 2012). Our RT-PCR and qPCR results demonstrated that the expression of P2X₇ mRNA in gp120-treated groups increased statistically compared to that of the control group, indicating that gp120 might induce the upregulation of P2X₇ mRNA.

Brain microglia, astrocytes, and innate immune cells of the brain parenchyma are responsible for homeostasis in normal CNS tissue, and are likely affected by ADC as excessive activation of microglial cells can induce CNS injury and neurodegenerative disease (Tambuyzer et al., 2009; Harry 2013; Hornik et al., 2014; Mosher and Wyss-Coray 2014). The P2X₇ receptor plays a major role in the regulation of microglia activity and is involved in inflammation and immune responses, and as such has an important role in neurodegenerative disease (Le Feuvre et al., 2002; Baudalet et al., 2015). Immunohistochemistry and western blot results demonstrated that ICV perfusion of gp120 significantly increased P2X₇ protein expression in the hippocampus of rats, suggesting that gp120 can induce the upregulation of P2X₇ receptor. Therefore, P2X₇ receptors are likely to be involved in the pathogenesis of learning and memory deficits induced by gp120 in rats. As such, the P2X₇ receptor might be closely associated with ADC. We investigated only the role of P2X₇ receptor in gp120-induced learning and memory deficits in the whole animal level, and the specific underlying mechanisms require further research. For instance, gp120 could specifically activate microglia cells in the hippocampus to influence others cells such as neurons, or inflammatory factors (for example, TNF α and IL-1 β), superoxide (for example, NO and ROS) and NF- κ B could be involved in the regulation of P2X₇ receptor. The above hypotheses will be the basis of future research.

CONCLUSION

In this study, we found that gp120 treatment could successfully mimic HAD via ICV infusion in rats, and that P2X₇ receptor is involved in gp120-induced learning and memory deficits in rats. Our observations may further elucidate the relationship between P2X₇ receptors and ADC pathogenesis, which represents a novel target for prevention and treatment of ADC. There were some limitations to this project, and the specific mechanism of this interaction requires further researched.

Conflicts of interest

The authors declare no conflict of interest.

ACKNOWLEDGMENTS

Research supported by a grant (#GJJ14146) from the Youth Science Foundation of the Educational Department of Jiangxi Province, a grant (#20153BCB23033) from the Cultivating Foundation of Young Scientists of Jiangxi Province, and grants (#YC2014-S098 and #YC2015-S040) from the Innovation Foundation of the Graduate School of Jiangxi Province.

REFERENCES

- Arulkumaran N, Unwin RJ and Tam FW (2011). A potential therapeutic role for P2X7 receptor (P2X7R) antagonists in the treatment of inflammatory diseases. *Expert Opin. Investig. Drugs* 20: 897-915. <http://dx.doi.org/10.1517/13543784.2011.578068>
- Bachani M, Sacktor N, McArthur JC, Nath A, et al. (2013). Detection of anti-tat antibodies in CSF of individuals with HIV-associated neurocognitive disorders. *J. Neurovirol.* 19: 82-88. <http://dx.doi.org/10.1007/s13365-012-0144-8>
- Bartesaghi A, Merk A, Borgnia MJ, Milne JL, et al. (2013). Prefusion structure of trimeric HIV-1 envelope glycoprotein determined by cryo-electron microscopy. *Nat. Struct. Mol. Biol.* 20: 1352-1357. <http://dx.doi.org/10.1038/nsmb.2711>
- Baudelet D, Lipka E, Millet R and Ghinet A (2015). Involvement of the P2X7 purinergic receptor in inflammation: an update of antagonists series since 2009 and their promising therapeutic potential. *Curr. Med. Chem.* 22: 713-729. <http://dx.doi.org/10.2174/0929867322666141212120926>
- Bodner A, Maroney AC, Finn JP, Ghadge G, et al. (2002). Mixed lineage kinase 3 mediates gp120IIIB-induced neurotoxicity. *J. Neurochem.* 82: 1424-1434. <http://dx.doi.org/10.1046/j.1471-4159.2002.01088.x>
- Burnstock G (2009). Purinergic receptors and pain. *Curr. Pharm. Des.* 15: 1717-1735. <http://dx.doi.org/10.2174/138161209788186335>
- Chen L, Liu J, Xu C, Keblesh J, et al. (2011). HIV-1gp120 induces neuronal apoptosis through enhancement of 4-aminopyridine-sensitive outward K⁺ currents. *PLoS One* 6: e25994. <http://dx.doi.org/10.1371/journal.pone.0025994>
- Cunningham C (2013). Microglia and neurodegeneration: the role of systemic inflammation. *Glia* 61: 71-90. <http://dx.doi.org/10.1002/glia.22350>
- de Witte L, Bobardt M, Chatterji U, Degeest G, et al. (2007). Syndecan-3 is a dendritic cell-specific attachment receptor for HIV-1. *Proc. Natl. Acad. Sci. USA* 104: 19464-19469. <http://dx.doi.org/10.1073/pnas.0703747104>
- Dugas N, Dereuddre-Bosquet N, Goujard C, Dormont D, et al. (2000). Role of nitric oxide in the promoting effect of HIV type 1 infection and of gp120 envelope glycoprotein on interleukin 4-induced IgE production by normal human mononuclear cells. *AIDS Res. Hum. Retroviruses* 16: 251-258. <http://dx.doi.org/10.1089/088922200309340>
- Fields J, Dumaop W, Langford TD, Rockenstein E, et al. (2014). Role of neurotrophic factor alterations in the neurodegenerative process in HIV associated neurocognitive disorders. *J. Neuroimmune Pharmacol.* 9: 102-116. <http://dx.doi.org/10.1007/s11481-013-9520-2>
- Fornari RV, Wichmann R, Atsak P, Atucha E, et al. (2012). Rodent stereotaxic surgery and animal welfare outcome improvements for behavioral neuroscience. *J. Vis. Exp.* 59: e3528.
- Glass CK, Saijo K, Winner B, Marchetto MC, et al. (2010). Mechanisms underlying inflammation in neurodegeneration. *Cell* 140: 918-934. <http://dx.doi.org/10.1016/j.cell.2010.02.016>
- Gong Z, Yang L, Tang H, Pan R, et al. (2012). Protective effects of curcumin against human immunodeficiency virus 1 gp120 V3 loop-induced neuronal injury in rats. *Neural Regen. Res.* 7: 171-175.
- Harry GJ (2013). Microglia during development and aging. *Pharmacol. Ther.* 139: 313-326. <http://dx.doi.org/10.1016/j.pharmthera.2013.04.013>
- Hazleton JE, Berman JW and Eugenin EA (2010). Novel mechanisms of central nervous system damage in HIV infection. *HIV AIDS (Auckl.)* 2: 39-49.
- Hornik TC, Neniskyte U and Brown GC (2014). Inflammation induces multinucleation of Microglia via PKC inhibition of cytokinesis, generating highly phagocytic multinucleated giant cells. *J. Neurochem.* 128: 650-661. <http://dx.doi.org/10.1111/jnc.12477>
- Huang YH, Yen JC, Lee JJ, Liao JF, et al. (2015). P2X7 is involved in the anti-inflammation effects of levobupivacaine. *J. Surg. Res.* 193: 407-414. <http://dx.doi.org/10.1016/j.jss.2014.07.020>
- Keblesh JP, Dou H, Gendelman HE and Xiong H (2009). 4-Aminopyridine improves spatial memory in a murine model of HIV-1 encephalitis. *J. Neuroimmune Pharmacol.* 4: 317-327. <http://dx.doi.org/10.1007/s11481-009-9161-7>
- Krogh KA, Wydeven N, Wickman K and Thayer SA (2014). HIV-1 protein Tat produces biphasic changes in NMDA-evoked increases in intracellular Ca²⁺ concentration via activation of Src kinase and nitric oxide signaling pathways. *J. Neurochem.* 130: 642-656. <http://dx.doi.org/10.1111/jnc.12724>
- Le Feuvre R, Brough D and Rothwell N (2002). Extracellular ATP and P2X7 receptors in neurodegeneration. *Eur. J. Pharmacol.* 447: 261-269. [http://dx.doi.org/10.1016/S0014-2999\(02\)01848-4](http://dx.doi.org/10.1016/S0014-2999(02)01848-4)
- Maartens G, Celum C and Lewin SR (2014). HIV infection: epidemiology, pathogenesis, treatment, and prevention. *Lancet* 384: 258-271. [http://dx.doi.org/10.1016/S0140-6736\(14\)60164-1](http://dx.doi.org/10.1016/S0140-6736(14)60164-1)
- Mika A, Mazur GJ, Hoffman AN, Talboom JS, et al. (2012). Chronic stress impairs prefrontal cortex-dependent response inhibition and spatial working memory. *Behav. Neurosci.* 126: 605-619. <http://dx.doi.org/10.1037/a0029642>
- Mosher KI and Wyss-Coray T (2014). Microglial dysfunction in brain aging and Alzheimer's disease. *Biochem. Pharmacol.* 88: 594-604. <http://dx.doi.org/10.1016/j.bcp.2014.01.008>

- Ogden KK and Traynelis SF (2011). New advances in NMDA receptor pharmacology. *Trends Pharmacol. Sci.* 32: 726-733. <http://dx.doi.org/10.1016/j.tips.2011.08.003>
- Ortega F, Pérez-Sen R, Delicado EG and Teresa Miras-Portugal M (2011). ERK1/2 activation is involved in the neuroprotective action of P2Y₁₃ and P2X₇ receptors against glutamate excitotoxicity in cerebellar granule neurons. *Neuropharmacology* 61: 1210-1221. <http://dx.doi.org/10.1016/j.neuropharm.2011.07.010>
- Peluso MJ and Spudich S (2014). Treatment of HIV in the CNS: effects of antiretroviral therapy and the promise of non-antiretroviral therapeutics. *Curr. HIV/AIDS Rep.* 11: 353-362. <http://dx.doi.org/10.1007/s11904-014-0223-y>
- Potter MC, Figuera-Losada M, Rojas C and Slusher BS (2013). Targeting the glutamatergic system for the treatment of HIV-associated neurocognitive disorders. *J. Neuroimmune Pharmacol.* 8: 594-607. <http://dx.doi.org/10.1007/s11481-013-9442-z>
- Rosca EC, Rosca O, Simu M and Chirileanu RD (2012). HIV-associated neurocognitive disorders: a historical review. *Neurologist* 18: 64-67. <http://dx.doi.org/10.1097/NRL.0b013e318247bc7a>
- Ruelas DS and Greene WC (2013). An integrated overview of HIV-1 latency. *Cell* 155: 519-529. <http://dx.doi.org/10.1016/j.cell.2013.09.044>
- Sacktor N, Nakasujja N, Robertson K and Clifford DB (2007). HIV-associated cognitive impairment in sub-Saharan Africa—the potential effect of clade diversity. *Nat. Clin. Pract. Neurol.* 3: 436-443. <http://dx.doi.org/10.1038/ncpneuro0559>
- Singer EJ, Valdes-Sueiras M, Commins D and Levine A (2010). Neurologic presentations of AIDS. *Neurol. Clin.* 28: 253-275. <http://dx.doi.org/10.1016/j.ncl.2009.09.018>
- Surprenant A and North RA (2009). Signaling at purinergic P2X receptors. *Annu. Rev. Physiol.* 71: 333-359. <http://dx.doi.org/10.1146/annurev.physiol.70.113006.100630>
- Tambuyzer BR, Ponsaerts P and Nouwen EJ (2009). Microglia: gatekeepers of central nervous system immunology. *J. Leukoc. Biol.* 85: 352-370. <http://dx.doi.org/10.1189/jlb.0608385>
- Tang H, Lu D, Pan R, Qin X, et al. (2009). Curcumin improves spatial memory impairment induced by human immunodeficiency virus type 1 glycoprotein 120 V3 loop peptide in rats. *Life Sci.* 85: 1-10. <http://dx.doi.org/10.1016/j.lfs.2009.03.013>
- Thomas JB, Brier MR, Snyder AZ, Vaida FF, et al. (2013). Pathways to neurodegeneration: effects of HIV and aging on resting-state functional connectivity. *Neurology* 80: 1186-1193. <http://dx.doi.org/10.1212/WNL.0b013e318288792b>
- Trang T, Beggs S and Salter MW (2012). ATP receptors gate microglia signaling in neuropathic pain. *Exp. Neurol.* 234: 354-361. <http://dx.doi.org/10.1016/j.expneurol.2011.11.012>
- Yilmaz A, Price RW and Gisslén M (2012). Antiretroviral drug treatment of CNS HIV-1 infection. *J. Antimicrob. Chemother.* 67: 299-311. <http://dx.doi.org/10.1093/jac/dkr492>
- Zayyad Z and Spudich S (2015). Neuropathogenesis of HIV: from initial neuroinvasion to HIV-associated neurocognitive disorder (HAND). *Curr. HIV/AIDS Rep.* 12: 16-24. <http://dx.doi.org/10.1007/s11904-014-0255-3>
- Zhao L, Pu SS, Gao WH, Chi YY, et al. (2014). Effects of HIV-1 tat on secretion of TNF- α and IL-1 β by U87 cells in AIDS patients with or without AIDS dementia complex. *Biomed. Environ. Sci.* 27: 111-117.
- Zou J, Vetreno RP and Crews FT (2012). ATP-P2X₇ receptor signaling controls basal and TNF α -stimulated glial cell proliferation. *Glia* 60: 661-673. <http://dx.doi.org/10.1002/glia.22302>